

# Evaluation of Antiurolithiatic Effects of *Moringa oleifera* Lam. Leaves Extract: *In-vitro*, *in-silico* and *in-vivo* Approaches

Dose-Response:  
An International Journal  
October-December 2024:1–15  
© The Author(s) 2024  
Article reuse guidelines:  
[sagepub.com/journals-permissions](https://sagepub.com/journals-permissions)  
DOI: 10.1177/15593258241301222  
[journals.sagepub.com/home/dos](https://journals.sagepub.com/home/dos)



Hina Ali<sup>1</sup> , Qaiser Jabeen<sup>1</sup>, Ayesha Jamshed<sup>1</sup> , Syeda Abida Ejaz<sup>2</sup> , Maria Qadeer<sup>1</sup> , Mariya Anwaar<sup>1</sup> , and Hafiz Muhammad Farhan Rasheed<sup>1</sup>

## Abstract

**Objective:** *Moringa oleifera* Lam. (Moringaceae), has traditionally been used for various renal diseases including urolithiasis. Considering the therapeutic and nutritional values, the present study was designed to investigate the antiurolithiatic potential of *M. oleifera* leaves through *in-vitro*, *in-silico* and *in-vivo* approaches. **Methods:** Methanolic aqueous extract of *M. oleifera* leaves (MoL.Cr) was prepared and screened for phytoconstituents through FTIR and HPLC analysis, while antioxidant potential was determined by DPPH assay. Crystal nucleation, aggregation and growth assays were carried out to ascertain the *in-vitro* inhibitory effects of MoL.Cr. Molecular docking was performed to analyze the interactions between phytoconstituents and targeted proteins (Glycolate oxidase, Albumin and Tamm-Horsfall). Whereas, ethylene glycol-induced urolithiasis model (1% ammonium chloride +0.75% ethylene glycol) was used for *in-vivo* study. Presence of alkaloids, phenols, glycosides and flavonoids was confirmed by FTIR and HPLC analysis. **Results:** MoL.Cr significantly inhibited the CaOx crystal nucleation, aggregation as well as growth and normalized urinary and serum parameters. Histological studies showed that MoL.Cr significantly restored hyperoxaluria-induced irregular epithelial lining, interstitial inflammation and dilated proximal tubules. **Conclusions:** Thus, *M. oleifera* demonstrated marked stone inhibiting potential which can be due to its antioxidant, lowering of urinary concentration of stone forming constituents and anti-crystallization effects.

## Keywords

*Moringa oleifera* leaves, urolithiasis, glycolate oxidase, albumin, tamm-horsfall protein

## Introduction

Urolithiasis is a physiological abnormality in which stones are formed in any part of the urinary system including kidney, bladder and ureter.<sup>1</sup> The urinary stone formation includes supersaturation of urine, crystal nucleation, growth, accumulation and translocation to the surface of the renal epithelium.<sup>2</sup> An imbalance between urinary stone promoters (albumin, oxalate and uric acid) and stone-inhibitors (citrate, magnesium, nephrocalcin and urinary prothrombin fragment I) has been suggested as an important factor in the pathogenesis of renal calculi.<sup>3</sup> Kidney stones are classified on the basis of composition; i.e., calcium oxalate, calcium phosphate, uric acid, struvite and cystine stones. There are two main types of calcium oxalate (CaOx) crystals; i.e., calcium oxalate

monohydrate (COM) and calcium oxalate dihydrate (COD). Dendritic COM crystals with sharp edges that stick strongly to the renal epithelium and cause damage to epithelial tissue are a common manifestation of hyperoxaluria. The defense against

<sup>1</sup> Department of Pharmacology, Faculty of Pharmacy, the Islamia University of Bahawalpur, Bahawalpur, Pakistan

<sup>2</sup> Department of Pharmaceutical Chemistry, Faculty of Pharmacy, the Islamia University of Bahawalpur, Bahawalpur, Pakistan

Received 30 April 2024; accepted 24 October 2024

### Corresponding Author:

Hina Ali, Department of Pharmacology, Faculty of Pharmacy, the Islamia University of Bahawalpur, Bahawalpur 63100, Pakistan.  
Email: [hinakawn5@gmail.com](mailto:hinakawn5@gmail.com)



Creative Commons Non Commercial CC BY-NC: This article is distributed under the terms of the Creative Commons Attribution-NonCommercial 4.0 License (<https://creativecommons.org/licenses/by-nc/4.0/>) which permits non-commercial use, reproduction and distribution of the work without further permission provided the original work is attributed as specified on the SAGE

and Open Access pages (<https://us.sagepub.com/en-us/nam/open-access-at-sage>).

the retention of crystals that spontaneously form in the urine was proposed to include the preferential formation of COD crystals in the urine that prevent them from attaching to the renal tubular epithelium, reduce inflammation and calculogenesis.<sup>1,4</sup>

Urolithiasis is a medical challenge with a high rate of recurrence. Reports state that 10-12% of individuals in developed nations (10% of men and 3% of women) will experience a urinary stone at some point in their lives. The etiology of this disorder is multifactorial and involves various factors such as lack of physical activity, diet and genetics.<sup>5</sup> In addition to the physicochemical mechanism of stone formation (precipitation, growth and aggregation), the interaction between crystals and renal tubular epithelial cells is an important risk factor in renal stone formation. Supersaturation is also the driving force for crystallization in urine which leads to crystal nucleation. Urinary supersaturation, hyperoxaluria and hypercalciuria produce oxidative stress which may lead to cell apoptosis or necrosis. Thus, resultant cell injury and cell membrane damage cause the up-regulation of crystal-binding molecules (e.g., osteopontin) and enhance the binding ability of crystals to the cell membrane. After binding, crystals translocate into the interstitium and inflammation occurs which may lead to the release of monocyte that causes crystal adhesion or retention and stone formation.<sup>6</sup>

Though, various treatment options for the mitigation of urolithiasis developed over the years, variations occur regarding their clinical indications and effectiveness. Currently, urolithiasis treatment focus on reducing the stone recurrence rather than etiologies.<sup>7</sup> Plant-based remedies have been used during the ages to cure renal stones disease with quite beneficial outcomes. Therefore, it is valuable to use medicinal plants as a remedy to treat kidney stones.

One method of molecular modelling is protein and ligand docking. Predicting a ligand's (small molecule) position and orientation when it binds to an enzyme or protein receptor is the aim of protein-ligand docking. Many pharmaceutical companies have achieved significant advances in computer-aided drug design at several phases of drug development, including lead optimization, hit-to-lead molecule binding affinity enhancement and identification of new targets.<sup>8</sup> In the present study, various proteins such as glycolate oxidase, albumin and Tamm-Horsfall protein were targeted in the present study to evaluate the inhibitory effect of identified phytoconstituents.

*Moringa oleifera* Lam. is a rapidly growing softwood tree that belongs to the family Moringaceae. *M. oleifera* is indigenous to Pakistan, Afghanistan, Bangladesh and India, also found all over the world. It is known as a "Miracle tree" due to its nutritional values and "Mothers best friend" for its property to enhance milk production in lactating mothers. In 2007, it was reported that approximately 38% of adults in the USA had used *M. oleifera* as a natural herbal product for treatment of various ailments in previous years.<sup>9</sup>

It has been reported that leaves of *M. oleifera* have low calories, high concentrations of minerals, natural antioxidants and vitamins. Diuretic, lipid and blood pressure-lowering

properties of *M.oleifera* leaves are attributed to the presence of high polyunsaturated fatty acids and low saturated fatty acids content. Traditionally, it is also used for the improvement of skin and wound healing.<sup>10</sup> It is reported to have antimicrobial, antifungal, antibacterial, anti-inflammatory, antioxidant, antitumor, antifertility, hepatoprotective, antihypertensive, hypocholesterolemic, antiulcer, antipyretic, anti-diabetic, anticonvulsant and anti-allergic activities.<sup>11</sup>

Various parts of the plant such as dried root bark,<sup>12</sup> dried root wood,<sup>13</sup> fresh bark<sup>14</sup> and fresh pods<sup>15</sup> have already been reported against urolithiasis. Different species of *Moringa* including *Moringa oleifera* bark have also been reported for the modulation and inhibition of the crystallization process and crystal morphology of calcium oxalate monohydrate.<sup>16,17</sup> Despite the traditional use of *M. oleifera* leaves against renal disorders, and reported *in-vitro* crystallization antiurolithiatic potential,<sup>18</sup> no data is available for its use against the treatment of kidney stones. Therefore, the methanolic aqueous extract of *M. oleifera* leaves, an edible part, was considered for the investigation of effects against urolithiasis by employing various *in-vitro* crystallization studies, *in-vivo* and *in-silico* methods.

## Material and Methods

### Plant Material

Fresh leaves of *Moringa oleifera* Lam. were collected from Baghdad-ul-Jadeed campus, IUB and authenticated by the botanist, Mr. Abdul Hameed. The dried sample was deposited in the herbarium of Pharmacology research laboratory, department of Pharmacology, faculty of Pharmacy, IUB, Pakistan. Voucher numbers (MO-LE-10-20-170) was issued for future reference.

### Preparation of Crude Extract

5 kg leaves of *M. oleifera* Lam. were washed, cut into small pieces and then soaked in 80% methanolic aqueous solution. After 3 days, the plant material was filtered and soaked again. This procedure was repeated twice. After third filtration, the filtrate was subjected to evaporation to obtain a semi-solid paste. The prepared MoL.Cr was weighed, labelled and stored in freezer for future use.

### Chemicals

Analytical grade chemicals such as cystone (Himalaya, India), ammonium chloride (Lahore Pharma, Pakistan), calcium chloride dihydrate, sodium carbonate, sodium chloride, sodium oxalate, ethylene glycol (Merck, Germany), ketamine (Global Pharmaceutical, Pakistan), xylazine (MyLab, Pakistan), sodium acetate trihydrate (Duksan, Korea), hydrochloric acid (BDH, England), tris base (Fluka, USA) and formalin (Riedel-de Haen, Germany) were used in the study. Colorimetric assay kits were also used for the determination of

calcium, creatinine, magnesium, phosphorus, uric acid, urea and total protein (Human Diagnostic Worldwide, Germany) were also used.

### Phytochemical Screening

Phytochemical analysis was performed to confirm the presence of secondary metabolites like alkaloids, amino acids, carbohydrates, flavonoids, coumarins, glycosides, phenolic compounds, saponins, tannins and protein in MoL.Cr.<sup>19-21</sup>

### Antioxidant Assay

The antioxidant activity was performed, according to the method followed by Bashir and Gilani (2009) with minor modifications.<sup>22</sup> Using a methanolic solution of DPPH (2, 2-diphenyl-1-picrylhydrazyl), the antioxidant capacity MoL.Cr was assessed and compared with ascorbic acid (standard antioxidant). Various dilutions of MoL.Cr and ascorbic acid (5, 10, 25, 50, 75, 100, 125, and 150 µl/ml) were prepared in order to measure the DPPH free radical scavenging activity. After adding 1 mL of 0.1 mM DPPH solution to 3 mL of each dilution, the solutions were allowed to stand at room temperature for 30 minutes, and the absorbance at 517 nm was measured. The following formula was used to determine antioxidant potential:

$$\text{Percent DPPH radical scavenging} = [1 - (AA - AB) / AA] \times 100$$

AA = Absorbance of control and AB = Absorbance of sample.

### FTIR Analysis

IR analysis was carried out using FTIR spectrophotometer (Agilent Cary-630 ATR, USA).

### HPLC Analysis

Flavonoids, terpenoids, tannins and phenols were estimated using high-performance liquid chromatography (HPLC) method. During the experiment, standards (50 µg/mL) and MoL.Cr (10 mg/mL) solutions were prepared and left to stand at 4°C. The testing was performed on a Shimadzu LC10-AT VP Liquid Chromatograph with SIL-20A auto-sampler and SPD-10AV UV VIS detector. For separation, a Shim-Pack CLC-ODS (C-18, 25 cm × 4.6 mm, 5 µm) was used, which was kept at room temperature. The binary solvent system, consisting of solvent A (water: acetic acid-94:6, pH = 2.2) and solvent B (acetonitrile), was used as the mobile phase, with the following gradient elution: 15 minutes for 85% A: 15% B, 15-30 minutes for 55% A: 45% B, and 30-35 minutes for 0% A: 100% B. The flow rate was recorded; i.e., 1.0 mL/min and absorbance was measured at 280 nm.<sup>23</sup>

### In-vitro Crystallization Assay

*In-vitro* crystallization assay (nucleation, aggregation and crystal growth) was carried out in triplicate in compliance with the protocol followed by Jamshed et al (2022) and Mosquera et al (2020) with minor modifications.<sup>23,24</sup>

**Nucleation Assay.** In nucleation assay, the effects of MoL.Cr on CaOx crystallization was investigated. For this assay, 5 mM calcium chloride and 7.5 mM sodium oxalate solutions were prepared in a buffer (Tris-HCl, 0.05 M + NaCl, 0.15 M) having pH 6.5. Various dilutions of MoL.Cr and cystone (100-1000 µg) were prepared in distilled water. 20 µl of each dilution of MoL.Cr and cystone were mixed with 60 µl calcium chloride and then sodium oxalate (60 µl) was added in each dilution. These dilutions were incubated in oven (37°C) for 30 minutes. Then, after cooling the optical density was noted at 630 nm. Percent inhibition of crystal nucleation was calculated from the following formula:

$$\text{Percent Inhibition} = [1 - (\text{OD}(\text{Test}) / \text{OD}(\text{Control}))] \times 100$$

where, OD (test) is the optical density of cystone or MoL.Cr and OD (control) is the optical density of the negative control.

**Aggregation Assay.** The effects of MoL.Cr and cystone on the aggregation of crystals were studied by preparing the solution of 0.05 M calcium chloride and sodium oxalate, separately. After mixing the solutions, the mixture was heated in the water bath (60°C) for 60 minutes and then incubated overnight (37°C). After drying, 40 mg/50 mL crystals solution was prepared in a buffer (0.05 M Tris-HCl and 0.5 M NaCl) at pH 6.5. 20 µl of each dilution of MoL.Cr and cystone were mixed with 60 µl of CaOx crystals solution, incubated for 30 minutes and then optical density was recorded at 630 nm. Using the same formula as the nucleation assay, the percent inhibition of aggregation was computed.

**Crystal Growth Assay.** To determine the effects of MoL.Cr and cystone on crystal growth, various dilutions were prepared. 3 g/2 mL of CaOx slurry was made in sodium acetate (0.05 M) buffer at pH 5.7. Calcium chloride (0.004 M) and sodium oxalate (0.004 M) solutions were prepared and then 1 mL of each solution was mixed with a buffer (0.01 M HCl + 0.09 M NaCl) at pH 7.4. 30 µl of CaOx slurry was added to reaction mixture followed by addition of 1 mL each dilution of MoL.Cr and cystone. Then, optical density was measured at 214 nm for 10 minutes. The difference in OD was determined and then by using the formula percent inhibition of crystal growth was calculated.

### Molecular Docking Analysis

Molecular docking was performed to explore the interactions between phytoconstituents (quercetin and kaempferol) and targeted proteins. The 3D crystal structures of proteins namely

Glycolate oxidase, Albumin and Tamm-Horsfall protein were retrieved from the Protein Data Bank (<https://www.rcsb.com>) PDB IDs: 2RDT, 4JK4 and 4WRN).<sup>25</sup> Prior to docking analysis, the proteins were prepared using MGL tools,<sup>26</sup> by removing heteroatoms and water molecules followed by the addition of polar hydrogen atoms and kollman charges. After that protein structures were rendered and corrected for missing residues.<sup>27</sup> The docking protocol was validated by first separating the co-crystal ligand from the active pocket of the complex, and then redocking was performed to validate its accuracy.<sup>28</sup> During the validation procedure it was observed that RMSD values remained less than 2.0 Å, confirming the protocol is validated. After the validation, the 3D structure of quercetin and kaempferol was made by using ChemDraw 3D,<sup>29</sup> to get the most stable arrangement of atoms energy minimization was done. Docking analysis was performed with target protein using AutoDock's default genetic algorithm as the scoring function. The grid box dimensions were set as  $x = 25.323920$ ,  $y = 14.207116$ ,  $z = 20.050868$  for 2RDT,  $x = 63.837003$ ,  $y = 23.103888$ ,  $z = 32.965576$  for 4JK4 and  $x = -0.831054$ ,  $y = 47.246241$ ,  $z = 32.470409$  for 4WRN. The phytoconstituents were docked within the active pocket of target proteins, 100 different configurations were generated for each protein. The pose possessing most stable configuration with least binding energy was selected and analyzed in 2D and 3D positions using Discovery Studio visualizer version 16<sup>30</sup> to elaborate the interactions formed between synthesized compound and targeted proteins.

### Evaluation of In-vivo Antiuro lithiatic Potential of MoL.Cr

For the evaluation of antiuro lithiatic potential of MoL.Cr, ethylene glycol-induced urolithiasis model was used. The *in-vivo* study was performed after the approval by Pharmacy Animal Ethics Committee (PAEC) under the registration number PAEC/2020/27.

**Animals.** Adult male Wistar albino rats (150-270g) and Swiss mice (20-30g) were used in the experiment. The animals were allowed to acclimatize with the experimental conditions for 7 days before starting the experimental procedure.

**Sample Size.** The sample size or the number of animals in each group was measured by using power analysis method. This method is similar to the method used for calculation of sample size for clinical trials and clinical studies. Simple calculation was carried out manually with the help of formula and for complex calculations power analysis based software was used.<sup>31</sup>

$$\text{Sample size} = 2SD^2(Z^{\alpha/2} + 2^{\beta})^2/d^2$$

**Animal Model of Urolithiasis.** For the induction of kidney stones, 1% ammonium chloride (AC) and 0.75% ethylene glycol (EG) were administered in drinking water as a lithogenic treatment

for the first 5 days and then, only 0.75% EG was given for the next 16 day.<sup>32</sup>

After induction, animals were divided randomly into various groups with the same body for 21 days in drinking water. After 21 days, lithogenic treatment was discontinued. Normal control group and intoxicated group were given distilled water (5 mL/kg p.o.) per 24 h. One group was considered as standard group which received cystone (500 mg/kg p.o.) per 24 h, a standard drug. While, other groups were considered as treatment groups and treated with different doses of MoL.Cr; i.e., 100, 300 and 500 mg/kg for the next 14 days.

**Urine Collection and Analysis.** After the lithogenic treatment at 21<sup>st</sup> day and after the treatment with MoL.Cr at 35<sup>th</sup> day animals were placed in the metabolic cages individually for the collection of urine. Fresh 3 h morning urine samples were analyzed for the crystal count. For analysis, 1 mL of each urine sample was centrifuged at 3000 rpm for 5 minutes. After centrifugation, 950 µl of supernatant was removed and remaining portion was analyzed on a neubauer chamber under a light microscope. The number of crystals were counted as described previously.<sup>33</sup> Urinary crystals were semi-quantitatively analyzed using a scoring system; i.e., 0 = approximately no crystals, 1 = few crystals, 2 = several crystals and 3 = many crystals in urine.

After 24 h, urinary pH and urinary volume were determined. Uric acid, calcium, magnesium, phosphorus and total protein levels in urine were determined by using commercially available kits.

**Serum Analysis.** After the completion of study at 35<sup>th</sup> day, Animals were anesthetized with 0.2 mL/100 g ketamine/xylazine combination (10:1), intraperitoneally. Then, blood samples were collected through cardiac puncture and retro-orbital techniques. Blood samples were allowed to clot for 15 minutes and then centrifuged at 4000 rpm for 15 minutes.<sup>34</sup> Serums were analyzed for the determination of biochemical parameters; i.e., creatinine and blood urea nitrogen (BUN) by using commercially available kits.

### Kidney Histology

At 35<sup>th</sup> day, animals were sacrificed and one kidney of representative animal from each group was dissected out and preserved in 10% formalin and then histologically analyzed.

### Acute Toxicity Assay

Swiss albino mice of either sex (18-30 g) were divided into different groups comprising of five mice each to assess the toxicity of MoL.Cr as described previously.<sup>35</sup> Distilled water (10 mL/kg p.o.) was given to the normal control group. While, different doses of MoL.Cr; i.e., 0.3, 1, 3 and 10 g/kg, respectively were given to the remaining groups. The mice were observed critically for 2 h and then at the interval of 30 minutes for the next 6 h for any type of behavioral changes; i.e., alertness, convulsions, grooming, hyperactivity, salivation, urination, lacrimation, pain response, touch response, corneal reflex, writhing reflex,



gripping strength, righting reflex and skin color. Then, mortality rate of animals was observed for the next 48 h.

### Statistical Analysis

The values were expressed as Mean  $\pm$  SEM and results were statistically analyzed by using two-way ANOVA followed by Bonferroni's post hoc test. The data was analyzed by using Graphpad Prism version 08.

## Results

### Phytochemical and Antioxidant Screening of MoL.Cr

Phytochemical screening revealed the presence of alkaloids, saponins, flavonoids, phenolic contents, glycosides, tannins and coumarins in methanolic aqueous extract of MoL.Cr. Antioxidant assay demonstrated that at the concentration of 150  $\mu\text{g/ml}$ , MoL.Cr showed significant free radical scavenging activity; i.e.,  $92.19 \pm 0.3$  and results were comparable to the ascorbic acid ( $95.04 \pm 0.3$ ) [Figure 1](#).

### FTIR and HPLC Analysis

The major functional groups of MoL.Cr were identified and categorized by FTIR results based on transmittance band peak values and spectral features, as shown in [Figure 2](#).

The region from  $4000\text{--}1800\text{ cm}^{-1}$  revealed a broad peak at  $3255\text{ cm}^{-1}$ , indicating the presence of  $\text{--OH}$  stretching (hydroxyl or carboxylic acids) and  $\text{N-H}$  stretching (alkaloids). A minor peak at  $2927\text{ cm}^{-1}$  corresponded to the  $\text{C-H}$  stretching of the  $\text{--CH}_2$  group (terpenoids). The fingerprint region ( $1800\text{--}650\text{ cm}^{-1}$ ) identified secondary protein structures, phenolic compounds, terpenoids, alkaloids, and carbohydrates. The HPLC analysis of MoL.Cr indicated the presence of quercetin (Rt. 2.85 min), gallic acid (Rt. 4.28), caffeic acid (Rt.12.99), vanillic acid (Rt. 13.55), benzoic acid (Rt.14.82), chlorogenic acid (Rt.15.44), p-coumaric acid (Rt. 17.32), M-coumaric acid (Rt. 20.53) and sinapic acid as shown in [Figure 3](#) and [Table 1](#).

### Molecular Docking Analysis

[Figure 4](#) showing 2D and 3D binding interactions between quercetin within the active site of glycolate oxidase. The docking analysis depicts that amino acids residues LYS236 and ARG315 were found to have conventional hydrogen bonds with the quercetin with  $-9.7\text{ kJ/mol}$  energy as shown in [Table 2](#). Furthermore, amino acid residue HIS260 was found to have pi-pi stacked interaction with aromatic ring of quercetin.

Similarly, [Figure 5](#) describe the 2D and 3D binding interactions between Quercetin within the active pocket of Albumin. The docking study illustrates that amino acid residues LEU115, and LEU122 interact within the active pocket

of Albumin, forming pi-sigma and pi-alkyl linkage respectively which potentiate the binding interactions.

In [Figure 6](#), the 2D and 3D binding interactions were retrieved between Kaempferol within the active site of Tamm-Horsfall protein. The docking analysis states that amino acid THR685, GLY684, and SER683 formed 3 conventional hydrogen bonds with kaempferol. While CYS627 interact via pi-Sulphur interaction. Furthermore, the binding interaction was potentiated by amino acid residues ALA686, and CYS682 forming pi-alkyl linkage.

### In-vitro Crystallization Assay

The percent inhibition of nucleation, at highest concentration (1000  $\mu\text{g/ml}$ ) of MoL.Cr was found to be  $72 \pm 0.92\%$  as similar to cystone; i.e.,  $68.8 \pm 0.93\%$  ([Figure 7A](#)). The percent inhibition in aggregation assay for MoL.Cr was  $65.2 \pm 0.5\%$ ; whereas, cystone showed percent inhibition of  $69.8 \pm 0.60\%$ , at the concentration of 1000  $\mu\text{g/ml}$  ([Figure 7B](#)). The percent reduction of crystal growth in crystal growth assay was calculated to be  $66.33 \pm 0.3\%$  for 1000  $\mu\text{g/ml}$  as compared to cystone ; i.e.,  $69.7 \pm 0.33\%$  ([Figure 7C](#)).

### Evaluation of In-vivo Antiuro lithiatic Activity

Microscopic analysis of urine showed a significant ( $P < 0.001$ ) increase in the number and size of crystals in lithogenic rats as compared to the normal control group as depicted in [Figure 8](#). MoL.Cr showed dose-dependent effects and reduced the crystal count significantly ([Table 3](#)). According to the scoring system, normal control group showed no crystals, whereas, lithogenic rats showed many crystals. Treatment groups showed significant result at the doses of 100 (several crystals), 300 (many crystals) and 500 mg/kg (few crystals). Lithogenic treatment enhanced the urinary output. While, urine volume of MoL.Cr treated rats was significantly ( $P < 0.01$ ) less than the untreated group but greater than the normal control group. Lithogenic treatment caused significant ( $P < 0.001$ ) reduction in the urinary pH of intoxicated rats. MoL.Cr significantly restored the urinary pH dose-dependent and results were comparable to those of cystone ([table 3](#)).

Statistical analysis showed that lithogenic treatment significantly ( $P < 0.001$ ) enhanced the urinary uric acid, phosphorus and total protein levels as compared to the normal control group. MoL.Cr reduced the urinary uric acid, phosphorus and total protein levels in dose dependent-manners. Urinary calcium and magnesium levels were significantly ( $P < 0.001$ ) decreased in lithogenic rats at the dose of 500 mg/kg. MoL.Cr elevated urinary calcium and magnesium levels and results were almost comparable to that of cystone ([Figure 9](#)).

MoL.Cr caused significant reduction of serum creatinine and BUN levels at the doses of 300 ( $P < 0.01$ ) and 500 mg/kg ( $P < 0.001$ ) as compared to normal group, which were

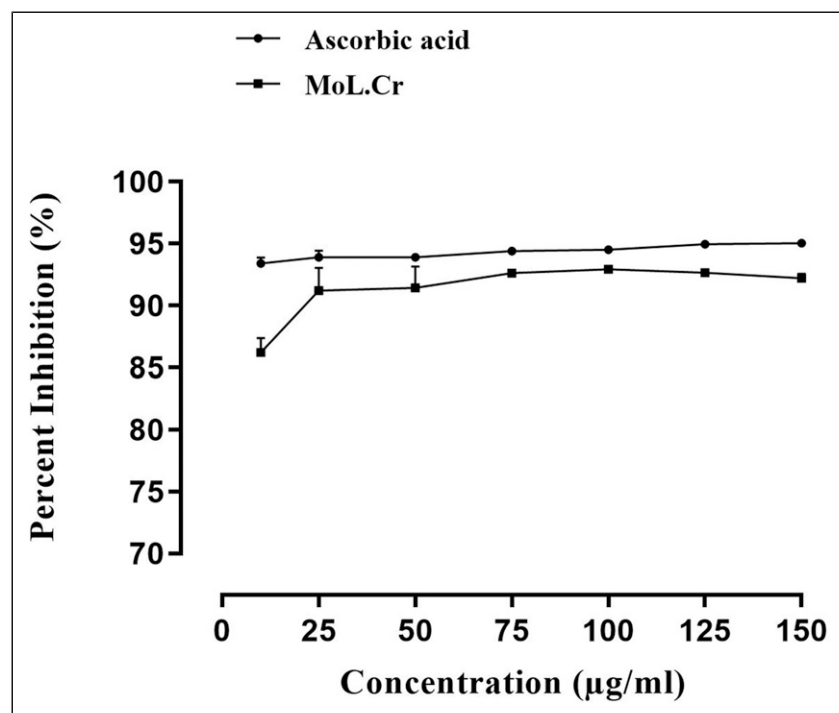


Figure 1. Antioxidant assay of MoL.Cr.

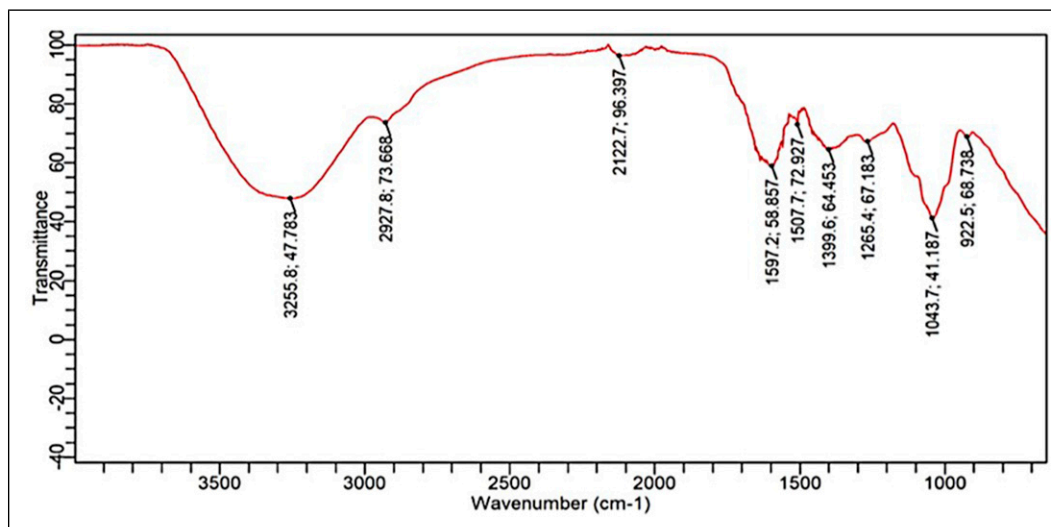


Figure 2. Representative FTIR spectra of MoL.Cr showing characteristic transmittance peaks of specific functional groups of phytoconstituents.

increased after the lithogenic treatment. Cystone showed same effects at the dose of 500 mg/kg (Figure 10).

### Histological Examination of Kidney

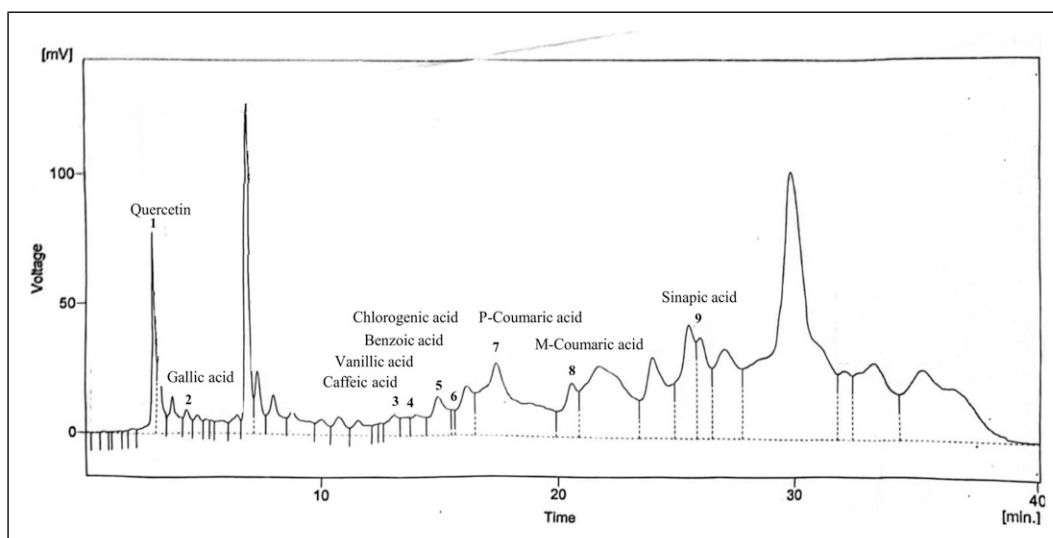
Histological examination showed no nephrotic damage in the normal control group. While, epithelial damage and disarrangement of nephrotic cell membrane were observed in lithogenic rats which were restored in MoL.Cr treated groups. MoL.Cr improved the structure of renal tubular epithelial cells dose-dependently (Figure 11).

### Acute Toxicity Assay

MoL.Cr was found safe upto the dose of 10 g/kg and no mortality, toxicity and behavioral changes were observed after 48 hours.

### Discussion

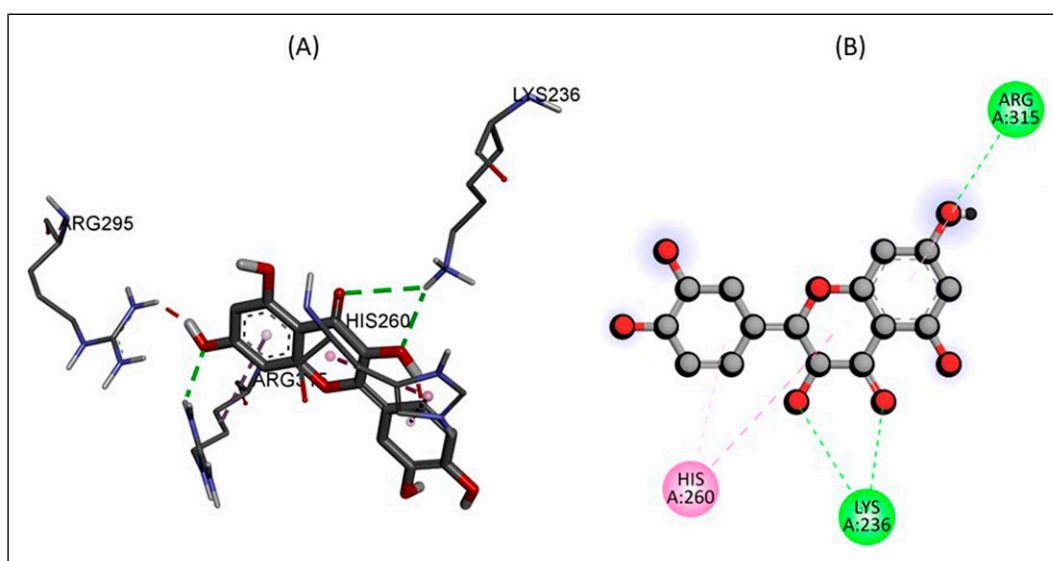
In the current study, the aqueous methanolic extract of *M. oleifera Lam.* leaves was evaluated to determine its effects against urolithiasis. As a tool for characterizing plant metabolites, FTIR



**Figure 3.** HPLC chromatogram of MoL.Cr indicating presence of phytochemical compounds.

**Table 1.** HPLC Profile of Phytochemical Compounds Detected in the MoL.Cr.

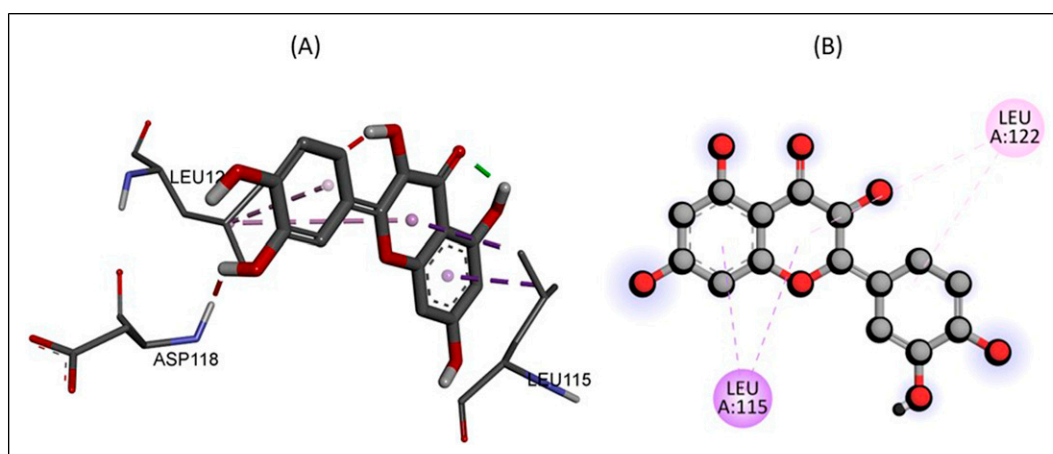
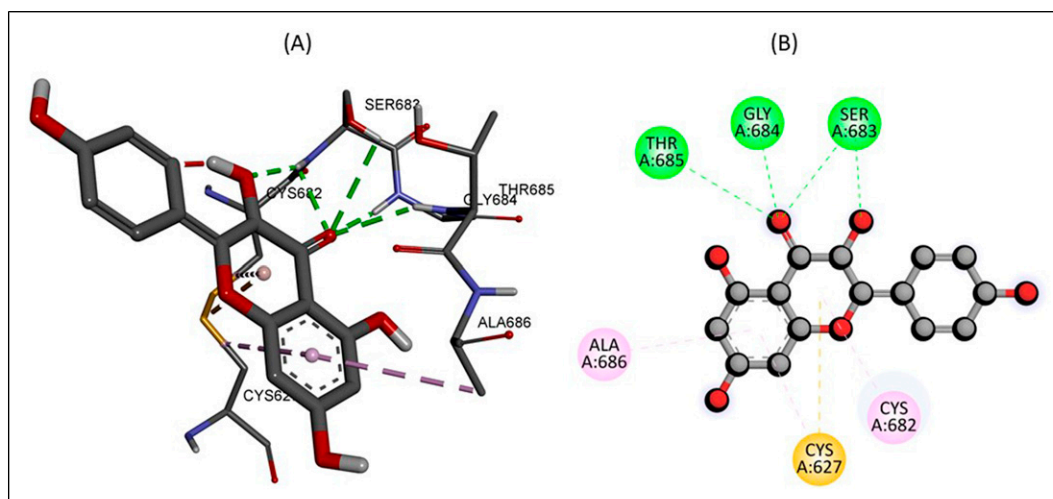
Phytochemical compounds	Retention time (min)	Area (%)	Concentration (ppm)
Quercetin	2.85	1.7	37.76
Gallic acid	4.28	0.4	6.18
Caffeic acid	12.99	0.6	12.15
Vanillic acid	13.55	0.4	10.66
Benzoic acid	14.82	1.6	70.59
Chlorogenic acid	15.44	0.2	7.83
p-Coumaric acid	17.32	7.7	42.99
M-Coumaric acid	20.53	2.1	10.89
Sinapic acid	26.0	3.1	17.36



**Figure 4.** The predicted 2D and 3D binding mode of Quercetin within the active site of Glycolate oxidase.

**Table 2.** Molecular Docking Scores of Compounds With Targeted Protein.

Compound	Protein	Binding energy kj/mol	Conventional hydrogen bonds	Hydrophobic interactions
Quercetin $C_{15}H_{10}O_7$	Glycolate oxidase (PDB ID: 2RDT)	-9.7	LYS236, ARG315	HIS260
Quercetin $C_{15}H_{10}O_7$	Albumin (PDB ID: 4JK4)	-8.2	No	LEU115, LEU122
Kaempferol $C_{15}H_{10}O_6$	Tamm-horsfall protein (PDB ID: 4WRN)	-8.1	THR685, GLY684, SER683	ALA686, CYS682, CYS627

**Figure 5.** The predicted 2D and 3D binding mode of Quercetin within the active site of Albumin.**Figure 6.** The predicted 2D and 3D binding mode of Kaempferol within the active site of Tamm-Horsfall protein.

spectroscopy has grown significantly, and it is currently regarded as one of the most accurate, sensitive, quick, non-destructive and affordable methods for identifying functional groups. The functional groups of the pharmacologically active components present in MoL.Cr was identified using FTIR analysis by interpreting the bands obtained in the infrared region, specifically the -OH (polyphenols). HPLC investigation of MoL.Cr showed that leaves of *M. oleifera* are a rich source of bioactive

compounds; i.e., quercetin, gallic acid, caffeic acid, vanillic acid, benzoic acid chlorogenic acid, p-coumaric acid, M-coumaric acid and sinapic acid. Previous studies have also reported the presence of flavonoids and phenolic acid that creates a positive link with its potential as an antiurolithiatic agent.<sup>36</sup> Flavonoids have been reported to diminish experimentally-induced urolithiasis in rats through numerous pathways such as modifying urinary stone-forming composition, reducing renal oxidative stress and



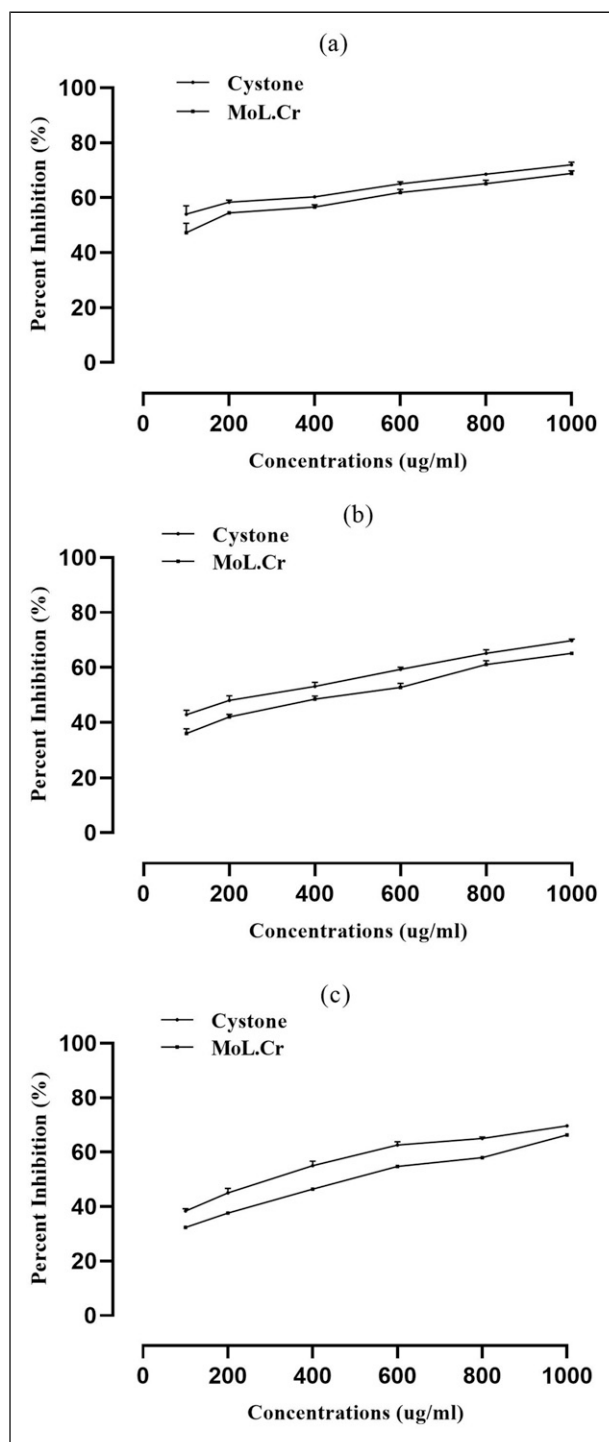


**Figure 7.** Inhibitory potential of MoL.Cr and cystone against calcium oxalate crystals; (A) nucleation assay, (B) aggregation assay and (C) crystal growth assay.

inflammatory damage. Terpenes have been known for their spasmolytic, calcium channel blocking, antioxidant and diuretic properties. It has been reported that leaves of *M. oleifera* possess a thiocarbamate glycoside named niazimicin, reported to possess spasmolytic potential that can be linked to medical expulsive

therapy (MET), used for the management of urolithiasis.<sup>37</sup> However, the potential of other phytochemical constituents against urolithiasis activity cannot be neglected.<sup>22,23</sup>

One of the main enzymes in oxalate production is glycolate oxidase (GOX). Through oxidation, it transforms glycolate into glyoxylate, which is further transformed into oxalate. Current molecular docking study showed that amino acids residues LYS236 and ARG315 were found to have conventional hydrogen bonds with the quercetin and are exclusively involved in the substrate binding and substrate specificity of glycolate oxidase enzymes. Mutations in these amino acids were discovered to diminish their catalytic activity.<sup>38</sup> Docking of Quercetin at the enzyme active site resulted in the lowest energy conformations ( $-9.7$  kJ/mol), indicating the best potential interactions between the ligands and active site residues. Albumin is the most abundant urinary protein that has been detected in the matrix of stones in humans. When exposed to metastable urinary solutions, albumin binds with calcium oxalate (CaOx) and uric acid crystals, and promotes crystal nucleation. Whereas, Tamm-Horsfall protein (THP), also known as uromucoid, is the most extensively investigated urinary macromolecule. THP acts as a first-line defense against kidney stone formation and acts as an effective inhibitor of crystal aggregations.<sup>6</sup> Results showed that quercetin and albumin showed best potential interaction with binding energy  $-8.2$  kJ/mol. Similarly, kaempferol and Tamm-Horsfall protein also showed the strong interaction with binding energy  $-8.1$  kJ/mol. Thus, this work revealed an intriguing breakthrough in the development of novel anti-GOX compounds.

*In-vitro* assays were carried out to investigate the nucleation, aggregation and growth phases of crystallization. The formation of loose clusters which may grow in size in the supersaturated urine containing ions and macromolecules with the addition of other molecules is the first step towards heterogeneous nucleation. Crystal aggregation, which ultimately results in crystal growth, starts as soon as the nucleus is anchored on the epithelial surface.<sup>23</sup> In *in-vitro* crystallization assays that involve CaOx crystal aggregation, nucleation and growth, were significantly inhibited by MoL.Cr. These *in-vitro* tests provide a rapid assessment of the antiurolithiatic, crystal-modifying activity and possible mechanism of actions. However, urolithiasis pathophysiology and biological system are complex, it is difficult and unsafe to extrapolate these *in-vitro* investigations for the therapeutic benefits. Consequently, the purpose of *in-vivo* urolithiasis models is to better understand the underlying mechanism of kidney stone formation and explore the potential of MoL.Cr against urolithiasis. After 21 days of lithogenic treatment, relatively large and abundant urinary crystals were found in lithogenic rats as compared to the normal control group. Ethylene glycol increases the urinary oxalate level, which is the major factor that promotes crystallization. In urine, elevated levels of oxalate form the complex with calcium and crystallization occur.<sup>39</sup> MoL.Cr and cystone significantly ( $P < 0.001$ ) reduced the crystal count in dose-dependent manners and showed almost similar results.

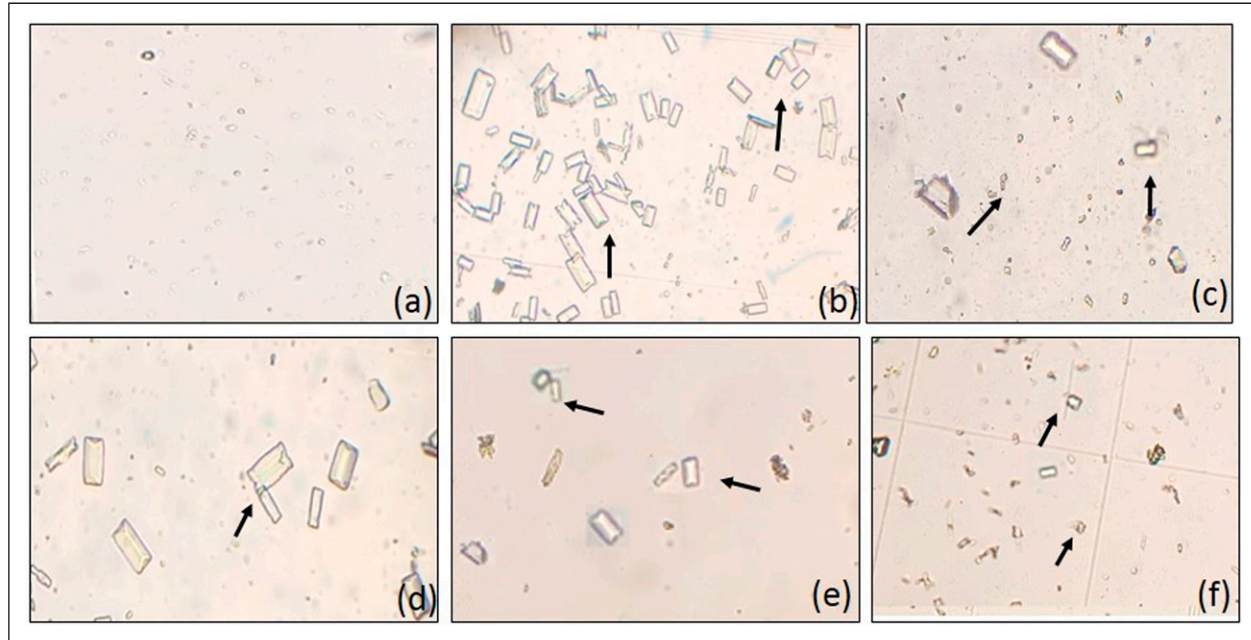


**Figure 8.** Microscopic images of urinary crystals (magnification 10×), curative model of urolithiasis (A) control, (B) intoxicated, (C) cystone (500 mg/kg), MoL.Cr; (D) 100 mg/kg, (E) 300 mg/kg and (F) 500 mg/kg, arrow(→)showing urinary crystals.

**Table 3.** Effects of MoL.Cr and Cystone on Urinary Crystal Count, Urinary Volume and pH in Curative Model of Urolithiasis.

Treatment	Crystal count/mm <sup>3</sup>		Urine volume (ml/100g)		Urinary pH	
	Day 21	Day 35	Day 21	Day 35	Day 21	Day 35
Control group	10.33 ± 1.2	9.2 ± 1.0	2.5 ± 0.1	2.4 ± 0.1	7.15 ± 0.2	7.2 ± 0.2
Intoxicated group	281 ± 5.2####	274.8 ± 4.4	5.3 ± 0.1####	5.1 ± 0.1	5.3 ± 0.2####	5.5 ± 0.3
MoL.Cr (100 mg/kg)	276.3 ± 3.6	256.5 ± 4.7 <sup>ns</sup>	4.9 ± 0.2	4.7 ± 0.2 <sup>ns</sup>	4.9 ± 0.2	5.4 ± 0.1 <sup>ns</sup>
MoL.Cr (300 mg/kg)	275.8 ± 4.5	247.3 ± 8.1**	5.0 ± 0.1	4.4 ± 0.1 <sup>ns</sup>	5.10 ± 0.3	6.3 ± 0.2**
MoL.Cr (500 mg/kg)	276.2 ± 4.6	210.8 ± 8.8***	5.2 ± 0.1	4.4 ± 0.1**	4.9 ± 0.2	7 ± 0.2***
Cystone (500 mg/kg)	277.5 ± 4.8	173.7 ± 4.2***	5.1 ± 0.1	3.4 ± 0.2***	4.9 ± 0.2	7.1 ± 0.1***

Mean ± SEM; n = 6.

ns:  $P > 0.05$ ; \*:  $P < 0.05$ ; \*\*:  $P < 0.01$ ; \*\*\*&####:  $P < 0.001$ .

(\*: Comparison within the groups; i.e., 21<sup>st</sup> and 35<sup>th</sup> day and #: comparison of intoxicated group with normal groups at 21<sup>st</sup> day; One-way ANOVA followed by bonferroni's post hoc test.

MoL.Cr significantly ( $P < 0.01$ ) restored the ethylene glycol-induced polyuria in intoxicated rats. Reabsorption of water in kidney decreases due to kidney stones as a result urine volume increases.<sup>34</sup> MoL.Cr and cystone restored the urine volume to a significant level but greater than untreated rats which may be due to the natural diuretic activity. Acidic pH favors the formation of calcium oxalate crystals (CaOx) in urine. Administration of ammonium chloride in lithogenic treatment makes the urine acidic and enhances the deposition of CaOx crystals. Whereas, calcium phosphate crystals are formed in alkaline pH.<sup>40</sup> MoL.Cr and cystone neutralized the urinary pH dose dependently as compared to the intoxicated rats and inhibited the crystal formation.

Urine analysis of lithogenic rats showed significantly increased levels of uric acid as compared to normal control

group. Uric acid decreases the solubility of CaOx crystals, binds with glycosaminoglycan and inhibits its stone inhibitory potential.<sup>24</sup> MoL.Cr treatment decreased the urinary uric acid levels and prevented the risk of stone formation and results were comparable to the cystone, the standard drug. Ethylene glycol-induced hyperoxaluria favors the complex formation of oxalate with calcium. After the complex formation, urinary excretion of calcium is decreased.<sup>40</sup> MoL.Cr restored the calcium levels in lithogenic rats, dose-dependently. Magnesium is considered a stone inhibitor as it inhibits the stone formation in the urinary system. Magnesium forms the complex with oxalate and enhances the solubility of CaOx crystals.<sup>41</sup> MoL.Cr is a rich source of magnesium and found to restore magnesium levels in lithogenic rats. Lithogenic treatment showed elevated levels of urinary phosphorus and

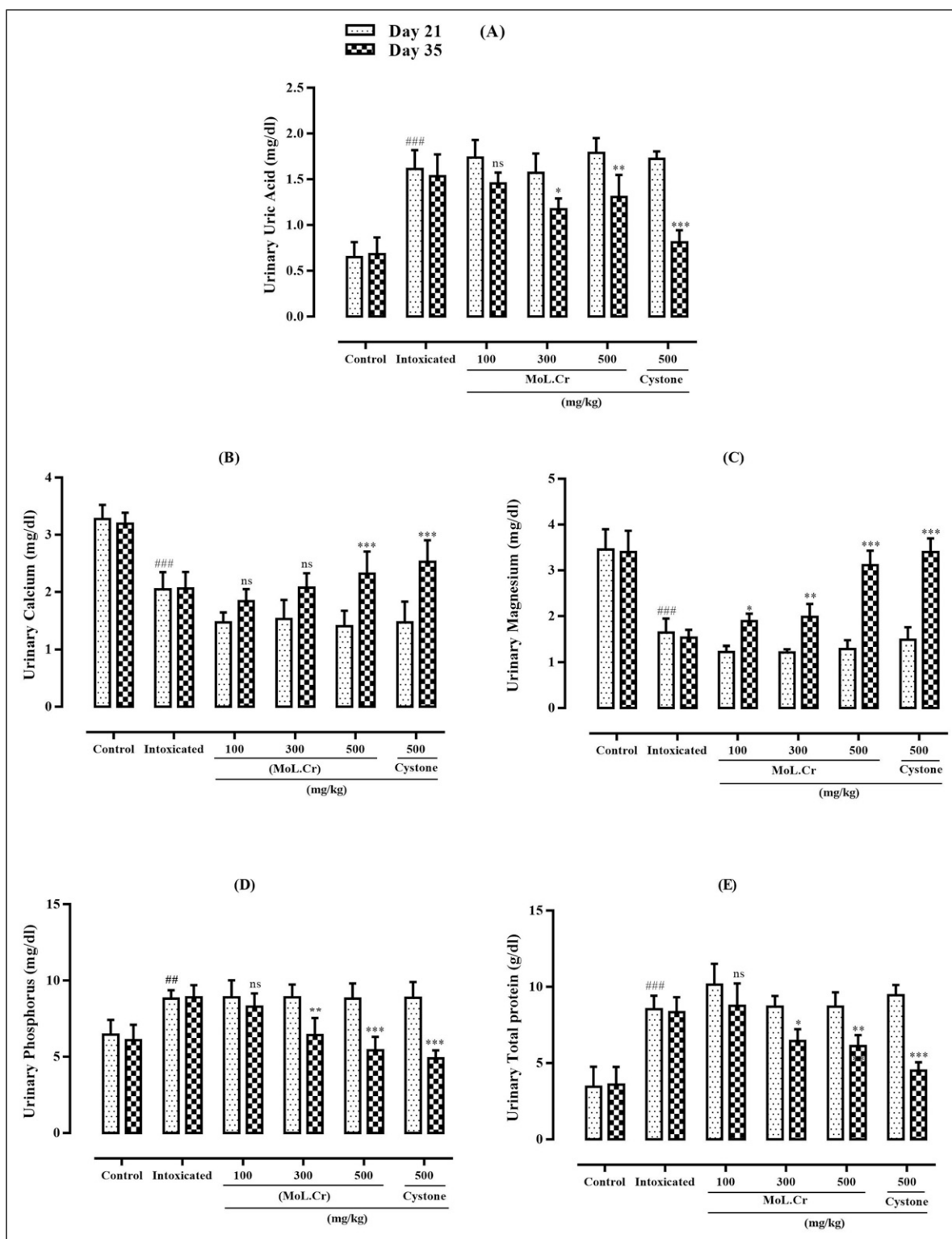


**Figure 9.** The effects of MoL.Cr and cystone on urine parameters (A) Uric acid, (B) Calcium, (C) Magnesium, (D) Phosphorus, (E) Total protein Mean  $\pm$  SEM; n = 6, ns:  $P > 0.05$ ; \*:  $P < 0.05$ ; ## & \*\*:  $P < 0.01$ ; \*\*\* & ####:  $P < 0.001$ . (\*: Comparison within the groups; i.e., 21<sup>st</sup> and 35<sup>th</sup> day and #: comparison of intoxicated group with normal groups at 21<sup>st</sup> day; One-way ANOVA followed by Bonferroni's post hoc test).

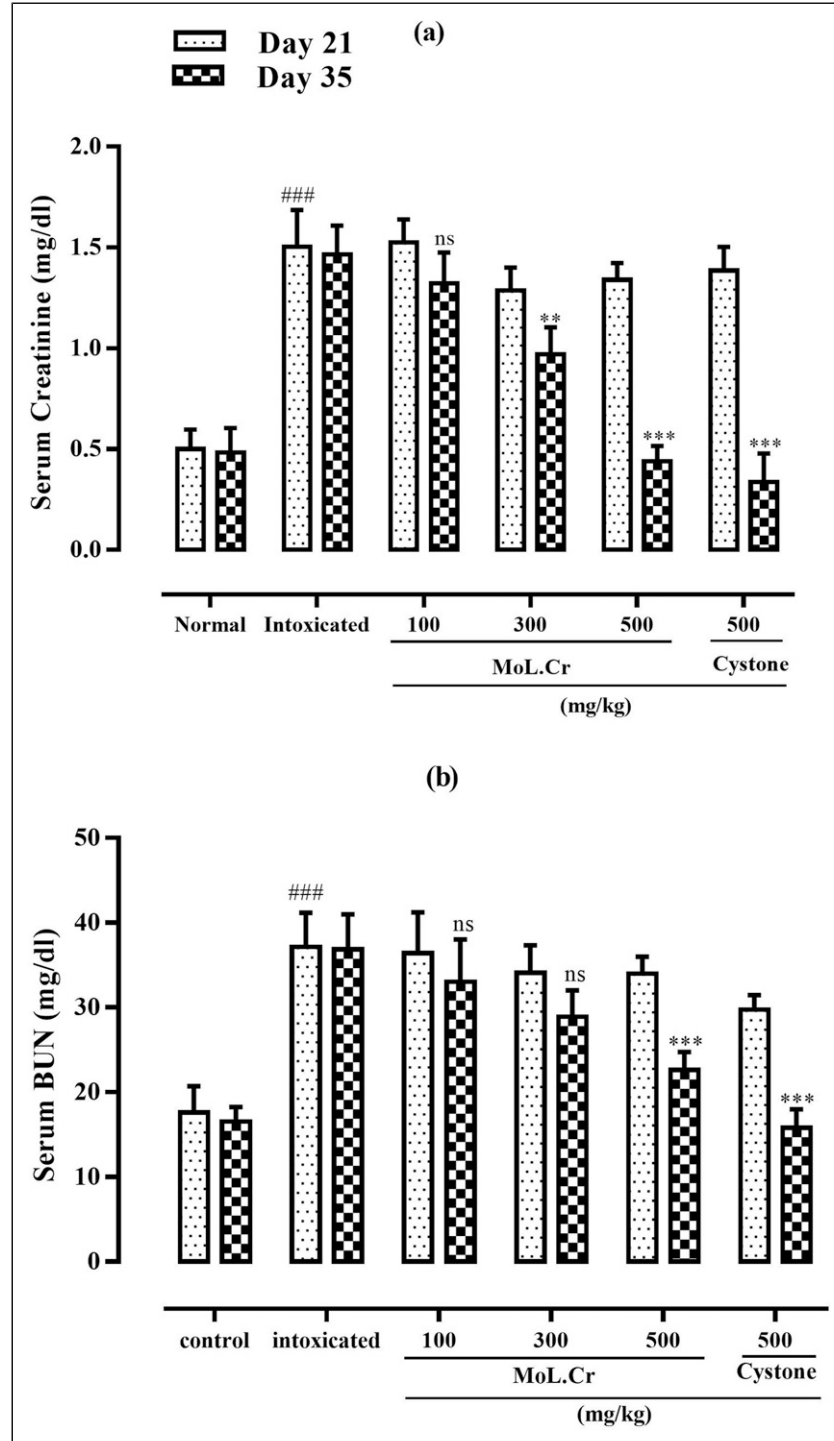


**Figure 10.** The effects of MoL.Cr and cystone on serum parameters (A) Creatinine, (B) Blood urea nitrogen (BUN). Mean  $\pm$  SEM; n = 6, ns:  $P > 0.05$ ; \*:  $P < 0.05$ ; \*\*:  $P < 0.01$ ; \*\*\*&####,  $P < 0.001$ . (\*: Comparison within the groups; i.e., 21<sup>st</sup> and 35<sup>th</sup> day and #: comparison of intoxicated group with normal groups at 21<sup>st</sup> day; One-way ANOVA followed by bonferroni's post hoc test).

total protein. Proteinuria indicates a high concentration of protein in urine due to kidney dysfunction. MoL.Cr and cystone reduced the phosphorus and total protein levels, significantly. In previous studies, it is reported that increased gene expression and production of molecules implicated in

inflammation and tissue remodeling were triggered by elevated phosphate levels, which formed an optimal situation for crystallization by producing calcium phosphate stones that epitaxially induce CaOx precipitation.<sup>41</sup> Treatment with MoL.Cr reduced phosphorus levels and reduced the risk of



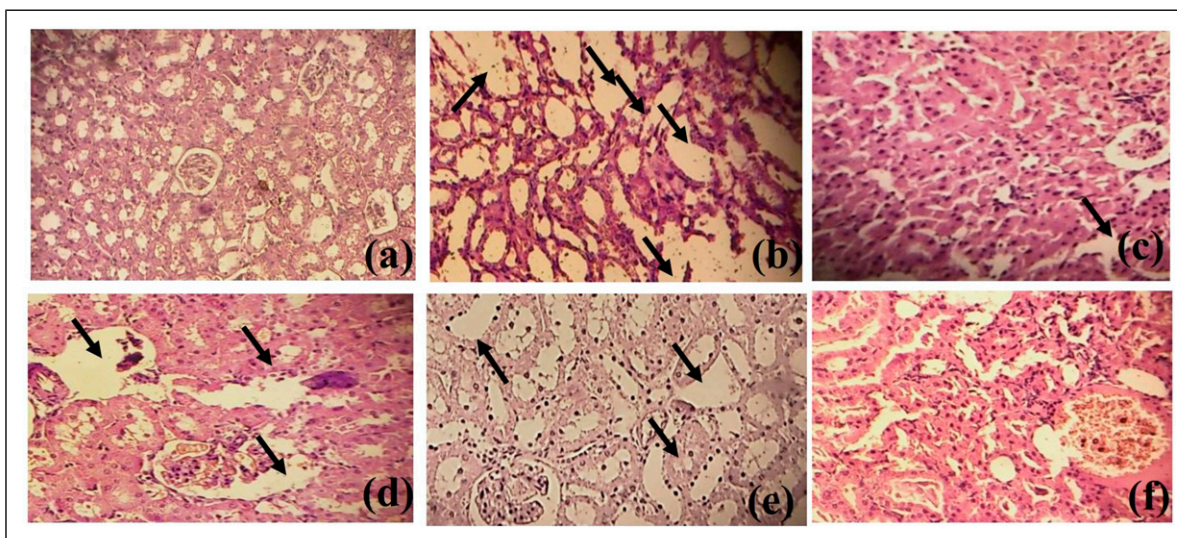


**Figure 11.** Histology of kidney (A) Normal control group (B) Intoxicated group (C) MoL.Cr; 100 mg/kg (D) MoL.Cr; 300 mg/kg (E) MoL.Cr; 500 mg/kg (F) Cystone; 500 mg/kg in curative model of urolithiasis. (↗: epithelium damage and disarrangement of nephrotic cell wall).

renal stones. The results of cystone and MoL.Cr were almost comparable to each other.

Kidney stones decrease the efficiency of glomerulus filtrate and also reduce urine filtration leading to the accumulation of nitrogenous substances such as creatinine and BUN in blood.<sup>24</sup> MoL.Cr and cystone showed pronounced effects and restored these parameters towards normal.

Histological examination of kidney section showed that lithogenic treatment disrupted the epithelial lining, dilated the proximal tubules and increased the interstitial spaces. Significant inflammation was observed in intoxicated rats which may be attributed to the high level of oxalate. MoL.Cr restored the renal tubular integrity in dose-dependent manners and reduced the crystal adhesion and attachment.

Results revealed that administration of MoL.Cr to urolithiatic rats decreased and inhibited the formation of urinary stones. Whereas, mechanism underlying these effects; determination of decreased urinary level of stone forming constituents, isolation and characterization of identified compounds and investigation of isolated compounds against urolithiasis are still unknown.

## Conclusions of the Study

The current study provided scientific validation for the traditional claim against kidney stone disease, demonstrating the curative potential of MoL.Cr against urolithiasis. Anti-urolithiatic effect of MoL.Cr may be mediated by a confluence of diuretic, antioxidant and crystal inhibitory effects. Additionally, MoL.Cr improved serum and urine biochemistry, providing a safer and more affordable option for the treatment of kidney stone disease.

## Acknowledgments

The authors acknowledge HEC (Higher Education Commission), Pakistan for support through NRP project, Number: 6300, in providing research animals.

## Declaration of conflicting interests

The author(s) declared no potential conflicts of interest with respect to the research, authorship, and/or publication of this article.

## Funding

The author(s) received no financial support for the research, authorship, and/or publication of this article.

## ORCID iDs

Hina Ali  <https://orcid.org/0000-0002-5474-7922>  
 Ayesha Jamshed  <https://orcid.org/0000-0001-7321-8754>  
 Syeda Abida Ejaz  <https://orcid.org/0000-0002-8516-7234>  
 Maria Qadeer  <https://orcid.org/0000-0001-6022-6405>  
 Mariya Anwaar  <https://orcid.org/0000-0002-7018-3581>  
 Hafiz Muhammad Farhan Rasheed  <https://orcid.org/0000-0003-2516-7387>

## References

1. Alomair MK, Alobaid AA, Almajed MAA, et al. Grape seed extract and urolithiasis: protection against oxidative stress and inflammation. *Phcog Mag.* 2023;19(1).
2. Liu Y, Liu Q, Wang X, et al. Inhibition of autophagy attenuated ethylene glycol induced crystals deposition and renal injury in a rat model of nephrolithiasis. *Kidney Blood Press Res.* 2018; 43(1):246-255.
3. Alelign T, Petros B. Kidney stone disease: an update on current concepts. *Adv Urol.* 2018;2018(1):3068365.



4. Khan SR. Crystal-induced inflammation of the kidneys: results from human studies, animal models, and tissue-culture studies. *Clin Exp Nephrol*. 2004;8:75-88.
5. Raj S, Rajan MSGS, Ramasamy S, et al. An in vitro Anti-Urolithiasis activity of a herbal formulation: *Spinacia oleracea* L. and *Coriandrum sativum* L. *Clinical Complement Med Pharmacol*. 2023;4(1):100124.
6. Aggarwal KP, Narula S, Kakkar M, Tandon C. Nephrolithiasis: molecular mechanism of renal stone formation and the critical role played by modulators. *BioMed Res Int*. 2013;2013:292953.
7. Ahmed OM, Ebaid H, El-Nahass E, Ragab M, Alhazza IM. Nephroprotective effect of *Pleurotus ostreatus* and *Agaricus bisporus* extracts and carvedilol on ethylene glycol-induced urolithiasis: roles of NF- $\kappa$ B, p53, bcl-2, bax and bak. *Biomolecules*. 2020;10(9):1317.
8. Mari KR, Muthukrishnan S. Structural characterization and insilico study on *Pisonia alba* Leaves extract. *J Pharmacogn Phytochem*. 2018;7(2):681-693.
9. Posmontier B. The medicinal qualities of *Moringa oleifera*. *Holist Nurs Pract*. 2011;25(2):80-87.
10. Meireles D, Gomes J, Lopes L, Hinzmann M, Machado J. A review of properties, nutritional and pharmaceutical applications of *Moringa oleifera*: integrative approach on conventional and traditional Asian medicine. *Advan Trad Med*. 2020;20:495-515.
11. Paikra BK, Dhongade HKJ, Gidwani B. Phytochemistry and pharmacology of *Moringa oleifera* Lam. *J Pharmacopuncture*. 2017;20(3):194-200.
12. Karadi RV, Palkar MB, Gaviraj EN, Gadge NB, Mannur VS, Alagawadi KR. Antiurolithiatic property of *Moringa oleifera* root bark. *Pharm Biol*. 2008;46(12):861-865.
13. Karadi RV, Gadge NB, Alagawadi KR, Savadi RV. Effect of *Moringa oleifera* Lam. root-wood on ethylene glycol induced urolithiasis in rats. *J Ethnopharmacol*. 2006;105(1-2):306-311.
14. Jameel F, Kumar MCS, Kodancha G, Adarsh B, Udupa AL, Rathnakar UP. Antiurolithiatic activity of aqueous extract of bark of *Moringa oleifera* (Lam.) in rats. *Health*. 2010;2(4):352-355.
15. Jameel F, Kumar MCS, Kodancha P, Benegal A, Udupa AL, Rathnakar UP. Antiurolithiatic activity of aqueous extract of *Moringa oleifera* (Lam.) pod in rats. *Pharmacologyonline*. 2010;3:716-721.
16. Menon S, Al-Saadi AS, Al-Aamri NJ, et al. Inhibition of crystallization of calcium oxalate monohydrate using leaves from different species of Moringa—Experimental and theoretical studies. *J Cryst Growth*. 2022;598:126859.
17. Menon S, Shinisha CB, Mamari HKA, et al. Experimental and theoretical studies on the modulation of the crystallization process and crystal morphology of calcium oxalate using *Moringa oleifera* bark extract. *J Mol Struct*. 2024;1305:137693.
18. Banik K, Akshitha S, Poojitha OV, Thulasi C, Vineetha V. Evaluation of antiurolithiatic activity of Moringa leaves by UV spectroscopic method. *Asian J Res Pharmaceut Sci*. 2020;10(3):141-144.
19. Agarwal K, Varma R. Radical scavenging ability and biochemical screening of a common Asian vegetable-*Raphanus sativus* L. *Int J Pharmaceut Sci Rev Res*. 2014;27(1):127-134.
20. Shaikh JR, Patil M. Qualitative tests for preliminary phytochemical screening: an overview. *Int J Chem Stud*. 2020;8(2):603-608.
21. Tiwari P, Kumar B, Kaur M, Kaur G, Kaur H. Phytochemical screening and extraction: a review. *Int Pharmaceut Sci*. 2011;1(1):98-106.
22. Bashir S, Gilani AH. Antiurolithic effect of *Bergenia ligulata* rhizome: an explanation of the underlying mechanisms. *J Ethnopharmacol*. 2009;122(1):106-116.
23. Jamshed A, Jabeen Q. Pharmacological evaluation of *Mentha piperita* against urolithiasis: an in vitro and in vivo study. *Dose Response*. 2022;20(1):15593258211073087.
24. Mosquera DMG, Ortega YH, Quero PC, Martínez RS, Pieters L. Antiurolithiatic activity of *Boldoa purpurascens* aqueous extract: an in vitro and in vivo study. *J Ethnopharmacol*. 2020;253:112691.
25. Bank PD. Protein data bank. *Nat New Biol*. 1971;233:223.
26. Huey R, Morris GM, Forli S. Using AutoDock 4 and AutoDock vina with AutoDockTools: a tutorial. *The Scripps Research Institute Molecular Graphics Laboratory*. 2012;10550(92037):1000.
27. Fattah TA, Saeed A, Al-Hiari YM, et al. Functionalized furo [3, 2-c] coumarins as anti-proliferative, anti-lipolytic, and anti-inflammatory compounds: synthesis and molecular docking studies. *J Mol Struct*. 2019;1179:390-400.
28. Attaullah HM, Ejaz SA, Channar PA, et al. Exploration of newly synthesized azo-thiohydantoins as the potential alkaline phosphatase inhibitors via advanced biochemical characterization and molecular modeling approaches. *BMC Chem*. 2024;18(1):47.
29. Brown T. ChemDraw. *Sci Teach*. 2014;81(2):67.
30. BIOVIA DS. BIOVIA discovery studio visualizer. *Software Version*. 2017;20:779.
31. Charan J, Kantharia N. How to calculate sample size in animal studies? *J Pharmacol Pharmacother*. 2013;4(4):303-306.
32. Atmani F, Slimani Y, Mimouni M, Hacht B. Prophylaxis of calcium oxalate stones by *Herniaria hirsuta* on experimentally induced nephrolithiasis in rats. *BJU Int*. 2003;92(1):137-140.
33. Khan A, Bashir S, Khan SR, Gilani AH. Antiurolithic activity of *Origanum vulgare* is mediated through multiple pathways. *BMC Complement Altern Med*. 2011;11(1):96.
34. Jamshed A, Jabeen Q. Prophylactic and curative potential of peppermint oil against calcium oxalate kidney stones. *Pak J Pharm Sci*. 2021;34(5):1867-1872.
35. Jabeen Q, Bashir S, Lyoussi B, Gilani AH. Coriander fruit exhibits gut modulatory, blood pressure lowering and diuretic activities. *J Ethnopharmacol*. 2009;122(1):123-130.
36. Saleem A, Saleem M, Akhtar MF, Ashraf Baig MMF, Rasul A. HPLC analysis, cytotoxicity, and safety study of *Moringa oleifera* Lam.(wild type) leaf extract. *J Food Biochem*. 2020;44(10):e13400.
37. Gilani AH, Aftab K, Suria A, et al. Pharmacological studies on hypotensive and spasmolytic activities of pure compounds from *Moringa oleifera*. *Phytother Res*. 1994;8(2):87-91.

38. Shirfule A, Sangamwar A, Khobragade C. Exploring glycolate oxidase (GOX) as an antiurolithic drug target: molecular modeling and in vitro inhibitor study. *Int J Biol Macromol.* 2011; 49(1):62-70.
39. Ali H, Nadeem A, Anwaar M, Jabeen Q. Evaluation of antiurolithic potential of *Moringa oleifera* seed extract. *Biomed J Sci Tech Res.* 2021;36(5):28889-28895.
40. Bashir S, Gilani AH. Antiurolithic effect of berberine is mediated through multiple pathways. *Eur J Pharmacol.* 2011; 651(1-3):168-175.
41. Divakar K, Pawar AT, Chandrasekhar SB, Dighe SB, Divakar G. Protective effect of the hydro-alcoholic extract of *Rubia cordifolia* roots against ethylene glycol induced urolithiasis in rats. *Food Chem Toxicol.* 2010;48(4):1013-1018.